Opposing roles for serotonin in cholinergic neurons of the ventral and dorsal striatum

Michael S. Virk[a,b,1,2], Yotam Sagi[a,1,2], Lucian Medrihan[a], Jenny Leung[a], Michael G. Kaplitt[c], and Paul Greengard[a,2]

[a]Laboratory of Molecular and Cellular Neuroscience, The Rockefeller University, New York, NY 10065; [b]Department of Neurosurgery, Weill Cornell Medical Center, New York, NY 10065; and [c]Laboratory of Molecular Neurosurgery, Weill Medical College of Cornell University, New York, NY 10065

Contributed by Paul Greengard, December 8, 2015 (sent for review November 9, 2015; reviewed by Floyd Bloom and Richard L. Huganir)

Little is known about the molecular similarities and differences between neurons in the ventral (vSt) and dorsal striatum (dSt) and their physiological implications. In the vSt, serotonin [5-Hydroxytryptamine (5-HT)] modulates mood control and pleasure response, whereas in the dSt, 5-HT regulates motor behavior. Here we show that, in mice, 5-HT depolarizes cholinergic interneurons (ChIs) of the dSt whereas hyperpolarizing ChIs from the vSt by acting on different 5-HT receptor isoforms. In the vSt, 5-HT1A (a postsynaptic receptor) and 5-HT1B (a presynaptic receptor) are highly expressed, and synergistically inhibit the excitability of ChIs. The inhibitory modulation by 5-HT1B, but not that by 5-HT1A, is mediated by p11, a protein associated with major depressive disorder. Specific deletion of 5-HT1B from cholinergic neurons results in impaired inhibition of ACh release in the vSt and in anhedonic-like behavior.

5-HT1A | 5-HT1B | cholinergic interneurons | ventral striatum | TRAP

Cholinergic interneurons (ChIs) represent only 1–2% of all striatal neurons (1). Despite their low abundance, ChIs play a major role in striatal function, by modulating both inputs to and outputs from spiny projection neurons (SPNs) (2). In the ventral striatum (vSt), ChIs are thought to play a major role in mediating reward, motivation, food intake, and hedonic behavior, whereas ChIs of the dorsal striatum (dSt) are implicated in motor behavior and action selection (3–5). Despite their functional differences, only a few morphological differences between vSt and dSt ChIs have been demonstrated, but no molecular differences between these two populations have been reported (6).

Serotonin [5-Hydroxytryptamine (5-HT)] signaling in the striatum has long been implicated in modulating locomotion as well as in mood control (7–9). Striatal 5-HT levels are high, and multiple 5-HT receptors (5-HTRs) are thought to mediate the function of 5-HT in these circuits (7, 10). In dSt ChIs, several 5-HTRs (5-HT7, 5-HT6, and 5-HT2) have been reported to induce membrane depolarization (11, 12), but the role of 5-HT signaling in vSt ChIs and its implication for mood regulation are poorly understood. To elucidate the role of 5-HT in vSt ChIs, we used electrophysiological recordings, optogenetics, and cell type-specific gene expression analysis. We demonstrate that 5-HT1A and 5-HT1B synergistically inhibit the function of vSt ChIs. The effect of activation of 5-HT1B, but not that of 5-HT1A, is mediated by p11. Furthermore, deletion of 5-HT1B from cholinergic neurons resulted in a loss of pleasure response (anhedonia), a core symptom of major depressive disorder.

Results

Opposite Effects of 5-HT on Cell Excitability Between vSt ChIs and dSt ChIs. To investigate the effect of 5-HT on ChIs from the vSt and dSt, we carried out electrophysiological recordings from visually identified neurons in acute brain slices. To identify ChIs, we used translating ribosome affinity purification (TRAP) mice expressing a GFP-tagged ribosomal protein, L10a, under the choline acetyltransferase promoter (13). GFP-positive cells demonstrated electrophysiological criteria of large afterhyperpolarization potential (AHP) and hyperpolarization-activated cation current (I_h), in line with the well-established characteristics of ChIs (14). Perforated-patch recordings in current-clamp configuration from ChIs in the vSt showed that bath application of 30 μM 5-HT decreased the tonic firing frequency from 0.9 ± 0.11 to 0.1 ± 0.06 Hz ($P = 0.0006$) and hyperpolarized the membrane potential from −53.8 ± 0.82 to −59.1 ± 0.86 mV ($P < 0.0001$) (Fig. 1 *A*, *C*, and *D*). On the contrary, the same treatment of 5-HT in the dSt increased the firing frequency of ChIs from 0.2 ± 0.06 to 1.4 ± 0.35 Hz ($P = 0.003$) and depolarized their membrane potential from −57.5 ± 0.77 to −54.7 ± 0.74 mV ($P < 0.0001$) (Fig. 1 *B*, *E*, and *F*).

To identify the 5-HTR isoforms that are present in vSt and dSt ChIs, we used TRAP and compared the level of the translated mRNA of 5-HTRs in these two neuronal populations. To this end, we immunoprecipitated tagged ribosomes from either dorsal or ventral portions of striatal slices. Nine genes of the 5-HTR family were detected in striatal ChIs (Fig. 1*H*). Four of these genes were differentially expressed between vSt and dSt ChIs (Fig. 1*G*). The highest expression level in vSt ChIs was that of *htr1b* [1.5 ± 0.29% of glyceraldehyde 3-phosphate dehydrogenase (*gapdh*) the housekeeping gene]. The level of this gene was 9.4-fold higher in vSt ChIs compared with dSt ChIs (0.16 ± 0.02% of *gapdh*, $P = 0.037$; Fig. 1*G*). Likewise, the expression level of *htr1a* in vSt ChIs was 7.0-fold higher than in dSt ChIs (0.7 ± 0.18% and 0.1 ± 0.02% of *gapdh* in vSt and dSt ChIs, respectively, $P = 0.024$). In contrast, the expression levels of the genes for choline acetyltransferase and vesicular acetylcholine (ACh) transporter were expressed at similar levels in both ChI populations (Fig. 1*I*). *htr7* level was 42-fold lower in vSt ChIs, relative to dSt ChIs (0.02 ± 0.05% and 0.84 ± 0.10% of *gapdh* in vSt and dSt ChIs, respectively, $P = 0.003$; Fig. 1*G*). 5-HT7 was previously suggested to mediate depolarization in dSt ChIs (11). *htr5a* level was 3-fold lower in vSt ChIs relative to dSt ChIs

Significance

The ventral striatum (vSt) and dorsal striatum (dSt) take part in different neuronal circuits that mediate emotional and motoric behaviors, respectively. vSt and dSt are populated by similar types of neurons, and little is known about the molecular differences between neurons of these regions. We report here that, in mice, serotonin [5-Hydroxytryptamine (5-HT)] oppositely regulates the excitability of cholinergic interneurons of the vSt and dSt. Postsynaptic 5-HT1A receptors and presynaptic 5-HT1B receptors synergistically mediate inhibition of ACh release from cholinergic neurons of the vSt. Deletion of 5-HT1B from cholinergic neurons resulted in an impairment in hedonic, but not motoric behavior. The present results contribute to our understanding of the specific functional roles of these brain areas.

Author contributions: M.S.V., Y.S., L.M., M.G.K., and P.G. designed research; M.S.V., Y.S., L.M., and J.L. performed research; M.S.V., Y.S., and L.M. analyzed data; and M.S.V., Y.S., L.M., M.G.K., and P.G. wrote the paper.

Reviewers: F.B., The Scripps Research Institute; and R.L.H., The Johns Hopkins University School of Medicine.

The authors declare no conflict of interest.

Freely available online through the PNAS open access option.

[1]M.S.V. and Y.S. contributed equally to this work.

[2]To whom correspondence may be addressed. Email: miv2010@nyp.org, ysagi@rockefeller.edu, or greengard@rockefeller.edu.

This article contains supporting information online at www.pnas.org/lookup/suppl/doi:10.1073/pnas.1524183113/-/DCSupplemental.

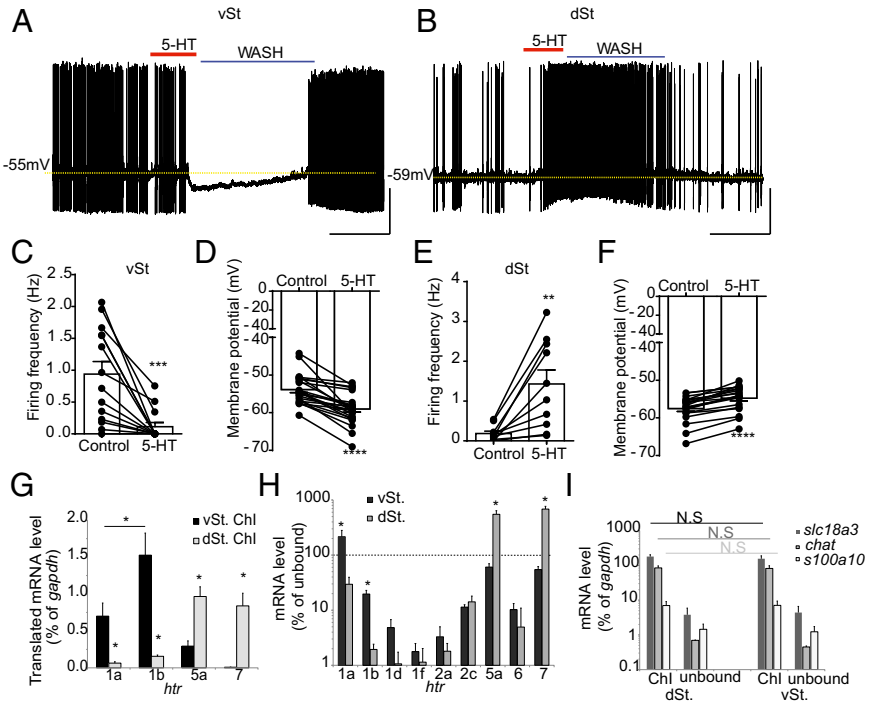

Fig. 1. 5-HT hyperpolarizes ChIs in the vSt and depolarizes ChIs in the dSt. (*A* and *B*) Perforated-patch recordings in current-clamp configuration from ChIs located in the (*A*) vSt and (*B*) dSt, demonstrating baseline tonic firing activity, 5-HT bath application (30 μM, 60 s), and subsequent washout. [Scale bars, 5 min (*x* axis) and 20 mV (y axis).] (*C–F*) ***$P < 0.001$, **$P < 0.01$, ****$P < 0.0001$ vs. control. Error bars in *C–F* represent SEM. Note that the dashed line represents the baseline resting membrane potential extrapolated from the control conditions. (*C* and *D*) vSt ChI firing frequency ($n = 14$ cells; *C*) and membrane potential ($n = 23$; *D*) in the presence of 5-HT (30 μM, 60 s). (*E* and *F*) dSt ChI firing frequency ($n = 10$; *E*) and membrane potential ($n = 20$; *F*) in the presence of 5-HT (30 μM, 60 s). (*G–I*) Bar graph summaries of mRNA levels in ChIs. (*G*) Bars represent mean mRNA levels as the percentage of *gapdh* ± SD ($n = 4$ samples per group; *$P < 0.05$ vs. vSt ChIs). (*H*) Bars represent mean mRNA levels as the percentage of that in the unbound fraction of the lysate ± SD (*$P < 0.05$ vs. unbound). Values above the dashed line represent enrichment in ChIs. (*I*) Bars represent mean mRNA levels as the percentage of *gapdh* ± SD (N.S, not significant).

(0.31 ± 0.05% and 0.97 ± 0.13% of *gapdh*, respectively, $P = 0.044$; Fig. 1*G*).

In addition to RNA from ChIs, we also isolated RNA from whole vSt and dSt tissues. We compared mRNA level from TRAP with that from the respective unbound fractions of the lysate. *htr1a* level in vSt ChIs was 2.3-fold higher relative to its level in that tissue (0.3 ± 0.01% of *gapdh* in vSt unbound, $P = 0.041$; Fig. 1*H*), suggesting that this gene is specifically enriched in ChIs. In contrast, *htr1b* level in vSt ChIs was 7.7-fold lower relative to that in the unbound tissue ($P = 0.027$; Fig. 1*H*), supporting the idea that 5-HT1B is present in SPNs (15, 16). *htr7* and *htr5a* levels in dSt ChIs were also 6.8- and 5.5-fold higher relative to their level in the nonspecific fraction, respectively, indicating that their expression in dSt ChIs is cell type-specific rather than tissue-specific (*htr7*, $P = 0.004$; *htr5a*, $P = 0.011$; Fig. 1*H*).

To validate the expression and localization of 5-HT1A and 5-HT1B proteins in striatal ChIs, we quantified the proportions of ChIs immunopositive for these 5-HTRs in vSt and dSt ChIs. Both 5-HT1A and 5-HT1B labeling was confirmed in vSt ChIs (Fig. 2 *A* and *B* and *SI Appendix*, Fig. S1). 5-HT1A immunolabeling was detected in 36 ± 6.8% of vSt ChIs but only in 3 ± 1.5% of dSt ChIs ($P = 0.029$). 5-HT1B staining was detected in 18 ± 7.9% of vSt ChIs but not in dSt ChIs (1 ± 1.9% of dSt ChIs, $P = 0.021$). 5-HT7 was expressed in 45 ± 11.9% of dSt ChIs but only in 14 ± 4.34% of vSt ChIs ($P = 0.028$; *SI Appendix*, Fig. S1). Due to the loose boundary between the vSt and the dSt, it is possible that 5-HT7–immunopositive cells that functionally relate to the dSt were attributed to the vSt. Interestingly, 5-HT5A immunolabeling was found in both populations (75 ± 7.9% of vSt ChIs and 78 ± 7.3% of dSt, $P = 0.886$; *SI Appendix*, Fig. S1).

5-HT1A and 5-HT1B are negatively coupled to adenylate cyclase activity (17), suggesting that they synergistically mediate the inhibitory response to 5-HT in vSt ChIs. We next used a pharmacological approach to validate that these 5-HTRs mediate the response to 5-HT in vSt ChIs. 5-HT1 agonists have been shown to inhibit ACh release from the vSt (18) and, indeed, bath application of the 5-HT1A agonist 8-OH-DPAT [8-hydroxy-2-(dipropylamino)tetralin; 10 μM] abolished the firing of vSt ChIs in perforated-patch recordings in the same manner as 5-HT (30 μM) (Fig. 2*C*). Moreover, subsequent bath application of the 5-HT1A antagonist WAY100635 (50–100 nM) reversed the firing rate of vSt ChIs to baseline conditions (Fig. 2*C*). In the presence of tetrodotoxin (TTX), 5-HT and 8-OH-DPAT hyperpolarized the membrane potential at similar levels, with 5-HT being on average more potent than 8-OH-DPAT (−5.8 ± 0.71 vs. −4.5 ± 0.67 mV, $P = 0.002$; Fig. 2 *D* and *F*), indicating that 5-HT1A receptors on vSt ChIs but not from other cells mediated this effect. Exposure to the 5-HT1A antagonist WAY100635 (50–100 nM) completely blocked the 8-OH-DPAT–induced hyperpolarization (Fig. 2 *E* and *F*) and abolished the response to subsequent application of 5-HT (0.84 ± 0.51 mV, $P < 0.0001$ vs. 5-HT; Fig. 2 *E* and *F*). On the other hand, the 5-HT1B agonist CP93129 (10 μM) had no effect on the vSt ChIs' somatic membrane potential (0.06 ± 0.21 mV, $P < 0.0001$ vs. 5-HT; Fig. 2 *E* and *F*), but this is not surprising, considering that these receptors are normally expressed only on the axon terminals (15).

5-HT1B and p11 Modulate ACh Efflux in the vSt. To further characterize the modulatory role of 5-HT in ChI activity, we measured ACh efflux in dialysates from freely moving mice (study design and histological analysis are illustrated in Fig. 3*A*). Increasing concentrations of neostigmine (100 nM–10 μM) elicited a steady efflux of ACh in a dose-dependent manner (Fig. 3 *B* and *C*). Neostigmine (1 μM) induced an efflux of 20.4 ± 7.51 fmol ACh/min in the vSt and 21.2 ± 8.93 fmol/min in the dSt ($P = 0.89$ between vSt and dSt; Fig. 3 *D–G*). Addition of TTX or exclusion of calcium from the solution completely abolished the effect induced by 10 μM neostigmine, further supporting the idea that this efflux was evoked by synaptic activity. Addition of 5-HT (5 μM) to the dialysis solution reduced ACh efflux in the vSt to 11.8 ± 5.59 fmol/min [$P = 0.029$ vs. artificial cerebrospinal fluid (aCSF); Fig. 3 *D* and *F*]. In contrast, dSt ACh efflux was increased by 5-HT (10 μM) to 34.7 ± 1.63 fmol/min ($P = 0.043$ vs. aCSF; Fig. 3 *E* and *G*), further supporting the idea that 5-HT oppositely regulates ChI function between the vSt and the dSt.

To directly study 5-HT signaling in vSt ChI function, we generated mice with deletion of 5-HT1B from cholinergic neurons [5-HT1B conditional knockout (cKO); *SI Appendix*, Fig. S2]. ACh efflux from the vSt of 5-HT1B cKO mice dialyzed with aCSF was 212% higher relative to that from WT littermates (43.3 ± 1.46 fmol/min, $P = 0.004$; Fig. 3*F*). In response to 5-HT, ACh efflux increased by 278% relative to WT (37.3 ± 8.37 fmol/min, $P = 0.026$; Fig. 3*F*). This increase in ACh release in the vSt may reflect a complete loss of the inhibition by 5-HT1B on tonically active vSt ChIs, without affecting the increase in the dSt by 5-HT. Because of the vertical positioning

NEUROSCIENCE

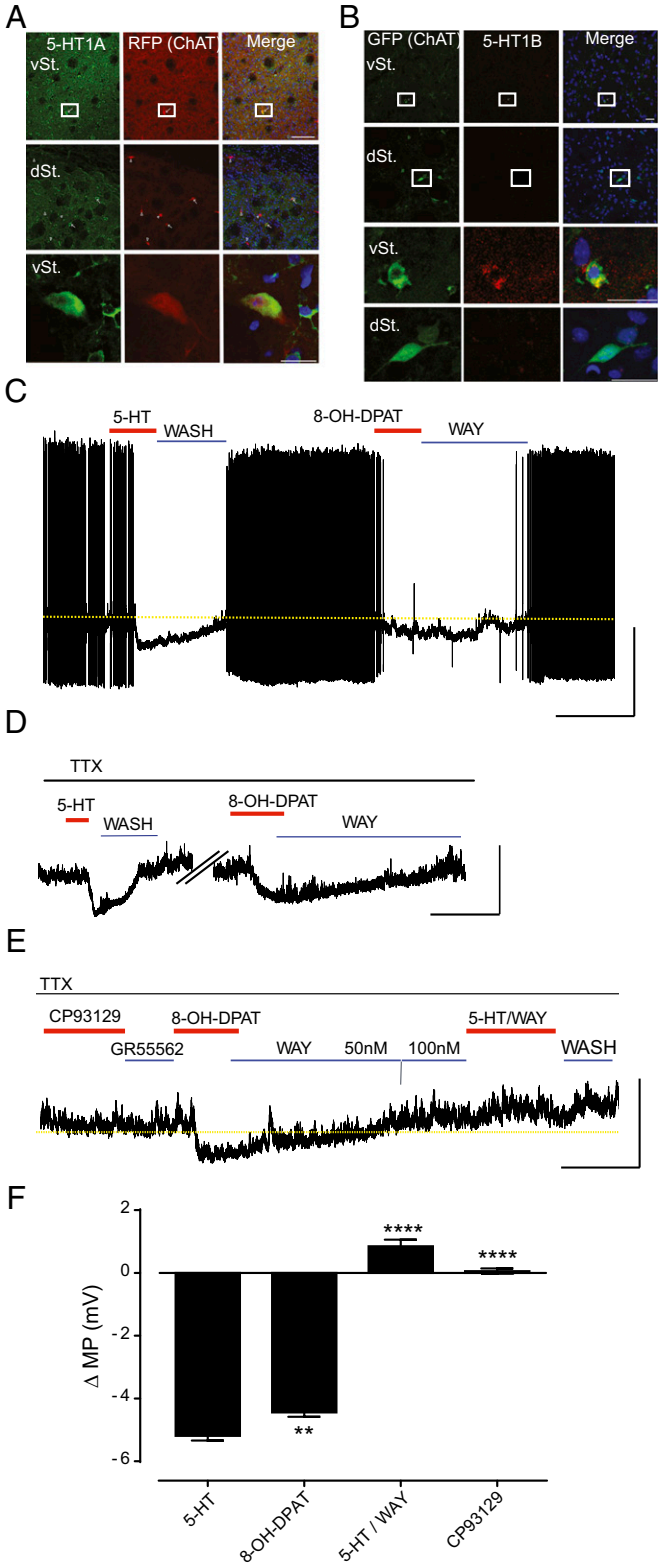

Fig. 2. 5-HT–induced hyperpolarization of vSt ChIs is mediated by 5-HT1A. (*A*) Representative immunolabeling images of 5-HT1A in the dSt and vSt of *ChAT*^{Cre}; *ROSA26*^{Tdtomato} mice. [Scale bars, 100 μm (boxes in top rows) and 20 μm (enlarged in bottom rows).] RFP, red fluorescent protein. (*B*) Representative immunolabeling images of 5-HT1B in the dSt and vSt of *ChAT*^{EGFP} ($n = 4$ mice). (Scale bars, 20 μm.) (*C*) Perforated-patch recording in current-clamp configuration from vSt ChIs demonstrating baseline tonic activity, 5-HT bath application (30 μM, 60 s) and washout, and 8-OH-DPAT (selective 5-HT1A agonist) bath application (10 μM, 2 min) followed by reversal with WAY100635 (selective 5-HT1A antagonist, 50–100 nM, 10 min). Note that the dashed line represents the baseline resting membrane potential extrapolated from the control conditions. [Scale bars, 5 min (*x* axis) and 20 mV (*y* axis).] (*D*) Membrane potential (MP) hyperpolarization induced by 5-HT (30 μM) and 8-OH-DPAT (10 μM) in the presence of TTX. [Scale bars, 5 min (*x* axis) and 10 mV (*y* axis).] (*E*) CP93129 (5-HT1B agonist) and GR55562 (5-HT1B antagonist) (both 10 μM/5 min) have no effect on MP, and 5-HT–induced hyperpolarization is completely blocked by pre-exposure to WAY100635. [Scale bars, 5 min (*x* axis) and 10 mV (*y* axis).] (*F*) Summary of ΔMP (mV) for vSt ChIs exposed to 5-HT ($n = 23$), 8-OH-DPAT ($n = 24$), and 5-HT following pre-exposure to WAY10635 ($n = 6$) and CP93129 ($n = 6$). Bars represent means ± SEM. $^{**}P < 0.01$, $^{****}P < 0.0001$ vs. 5-HT.

of the microdialysis probes, ACh released from both dSt and vSt is likely to be detected by the probe placed in the vSt, whereas probes placed in the dSt did not collect from the vSt. In line with this idea, baseline release of ACh as well as the response to 5-HT were unchanged in the dSt of 5-HT1B cKOs (Fig. 3*G*).

We recently identified a major role for the 11-kDa protein p11 in increasing the surface expression of 5-HT1B (19, 20). Translated mRNA level of p11 is highly enriched in ChIs (5), and was not different in dSt and vSt ChIs (7.1 ± 1.23% and 7.0 ± 1.45% of *gapdh* in vSt and dSt ChIs, respectively, $P = 0.84$; Fig. 1*I*). To elucidate the functional role of p11 in response to 5-HT in ChIs, we measured ACh efflux in mice with deletion of p11 from cholinergic neurons [p11 cKO mice (5)]. 5-HT increased ACh efflux in the vSt by 85% relative to aCSF (22.1 ± 4.49 fmol/min for aCSF and 40.9 ± 6.18 fmol/min for 5-HT, $P = 0.005$ vs. WT 5-HT; Fig. 3*F*). In contrast, the effect of 5-HT on dSt ChI activity as well as on the basal efflux in either territory was unchanged in p11cKO mice (Fig. 3 *F* and *G*), suggesting that p11 regulates the function of 5-HTRs in vSt ChIs but not in dSt ChIs. Because p11 mediates the heteroreceptor activity of 5-HT1B in glutamatergic nerve terminals and increases the surface expression of 5-HT1B (19–21), it is likely that the increase in ACh efflux in the vSt of p11 cKOs in response to 5-HT reflects a specific impairment in 5-HT1B function, without affecting that of 5-HT1A. In line with this idea, the hyperpolarizing effect of 5-HT on membrane potential or change in firing rate of vSt ChIs was not altered in p11 cKO mice (*SI Appendix*, Table S1). Together, these data strongly support the idea that 5-HT1B and p11 mediate the response to 5-HT in vSt ChIs.

5-HT1B and p11 Regulate Cholinergic Transmission in the vSt. To test whether 5-HT1B modulates synaptic output from vSt ChIs, we applied an optogenetic strategy in acute striatal slices. ACh release from ChIs increases the frequency of γ-aminobutyric acid type A ($GABA_A$) receptor-mediated spontaneous inhibitory postsynaptic currents (sIPSCs) in the neighboring neurons in several brain regions (3, 22–25). In our experiments, we used whole-cell patch-clamp recordings to monitor inhibitory postsynaptic currents in SPNs in acute vSt slices during optogenetic photostimulation of ChIs expressing modified channel rhodopsin (Fig. 4 *A* and *B* and *SI Appendix*, Fig. S3). Unlike the dSt, where optogenetic stimulation of ChIs evoked a synchronized GABA current mediated by dopaminergic terminals (25), in the vSt, light stimulation of ChIs increased the frequency of sIPSCs recorded in SPNs in a more asynchronous manner (*SI Appendix*, Fig. S4), as previously shown (3). In WT mice during a 20-Hz light stimulation of ChIs, comparable to the in vivo spiking activity of the vSt (26), the frequency of sIPSCs in SPNs was increased 1.45 ± 0.07 times ($P < 0.0001$) and this effect was abolished by the bath addition of the general muscarinic antagonist scopolamine (Fig. 4 *C* and *D*). On the contrary, the same stimulation protocol led to a 0.4 ± 0.06-fold decrease of the frequency of sIPSCs in SPNs from p11 cKO mice ($P < 0.0001$; Fig. 4 *C* and *D* and *SI Appendix*, Fig. S5), suggesting impairments in ACh signaling in the vSt of these mice.

Because 5-HT1B receptors are present on the axon terminals of ChIs and exert an inhibitory activity on neurotransmission (15, 18), next we used the same experimental protocol to investigate how

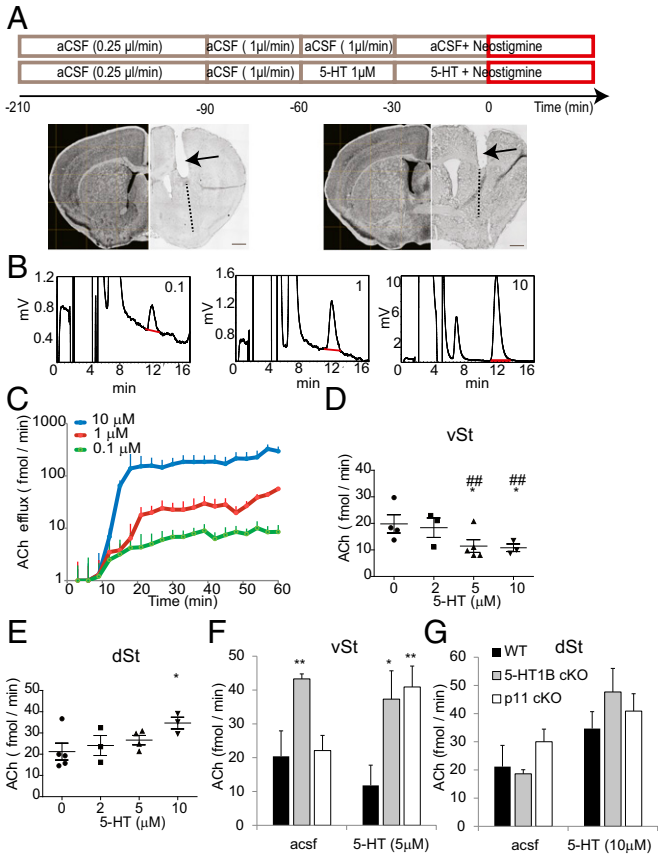

Fig. 3. 5-HT1B and p11 modulate ACh efflux in the vSt. (*A*) (*Top*) Experimental design. Three-minute intervals of dialysate collection started at time 0 min. (*Bottom*) Representative coronal sections showing the vSt (*Left*) and dSt (*Right*) after microdialysis. The arrows and dashed lines represent the location of the guiding cannula and the dialysis probe, respectively. (*Left*) Corresponding atlas images at Bregma +0.74 (vSt) and 0.0 mm (dSt) of the Mouse Brain Library Atlas (42). (Scale bars, 500 mm.) (*B*) Representative ACh chromatograms of individual samples from the dSt. aCSF was reverse-dialyzed with neostigmine. The number inside each box represents neostigmine concentration (µM). Note the red underlining indicating the ACh peak. (*C*) Quantitative summary of the experiment in *B*. Markers represent means ± SD ($n = 3$ mice). Mean efflux value between 21 and 36 min was used for statistical analysis. (*D* and *E*) Scatter dot plot analyses of ACh mean efflux values in the vSt (*D*) and dSt (*E*) following reverse dialysis with neostigmine (1 µM) without or with 5-HT (2–10 µM). Bars represent means ± SEM ($n = 3$–5 mice per group; $^{*}P < 0.05$ vs. aCSF; $^{\#\#}P < 0.01$ vs. dSt). (*F* and *G*) Bar graph summaries of ACh efflux in the vSt (*F*) and dSt (*G*) of WT (black), 5-HT1B cKO (gray), and p11 cKO mice (white). Bars represent mean efflux values ± SD ($n = 3$–5 mice per group; $^{*}P < 0.05$, $^{**}P < 0.01$ vs. WT).

pharmacological modulation of these receptors can influence ACh release from vSt ChIs. In WT mice, activation of the 5-HT1B receptors with their agonist CP93129 (10 µM) blocked the increase in the frequency of sIPSCs observed at baseline levels ($P = 0.004$; Fig. 4 *E* and *F*), whereas the addition of the 5-HT1B antagonist GR55562 (10 µM) further increased the frequency of sIPSC to 2.05 ± 0.27 times from baseline levels ($P = 0.006$; Fig. 4 *E* and *F*), indicating that 5-HT1B in the vSt inhibits ACh release from ChI terminals. However, in p11 cKO mice, addition of either the agonist or the antagonist of 5-HT1B receptor did not change the frequency ratio of sIPSCs in SPNs compared with baseline levels ($P = 0.991$ for CP93129 and $P = 0.960$ for GR55562; Fig. 4 *E* and *F*), suggesting that in vSt ChIs, presynaptic 5-HT1B receptors are not functional in the absence of p11.

5-HT1B Receptor in Cholinergic Neurons Regulates Hedonic Behavior. 5-HT1B dysfunction is linked to cognitive and emotional deficits (27, 28), but a specific neuronal type that mediates an antidepressant effect for 5-HT1B has not been suggested. We previously identified an antidepressant function for p11 (19), and recently we demonstrated that p11 in vSt ChIs contributes to its antidepressant action (5). Because p11 regulates 5-HT1B function in vSt ChIs, we decided to characterize the emotional and motoric behaviors of mice with selective deletion of 5-HT1B from cholinergic neurons (5-HT1B

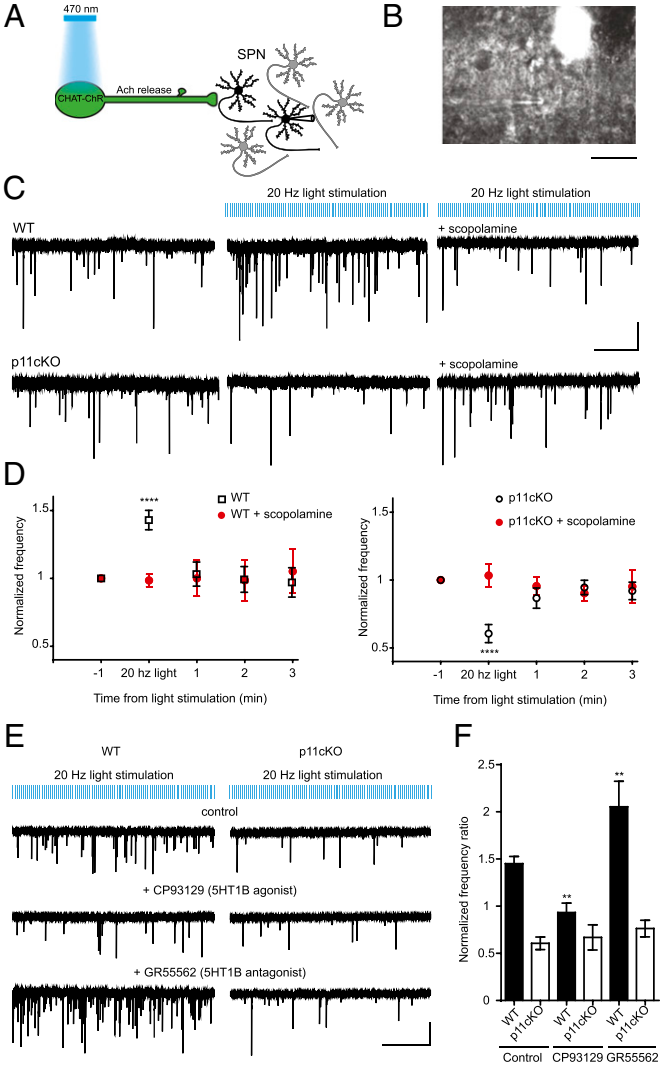

Fig. 4. Deletion of p11 disrupts the function of 5-HT1B receptors in vSt ChIs. (*A*–*C*) vSt ChIs infected with AAV9 containing E123T/H134R-ChR2-eYFP were activated by trains of blue light (470 nm) in acute slices, and sIPSCs from SPNs were recorded in the whole-cell patch-clamp configuration. (*B*) Image of a patch-clamped SPN and an adjacent fluorescent ChI in vSt. (Scale bar, 10 µm.) (*C*) Representative traces of sIPSCs recorded from SPNs in the vSt in WT (*Upper*) and p11cKO mice (*Lower*). (*Left*) Baseline activity of SPNs. (*Middle*) Traces recorded in constant 20-Hz light stimulation. (*Right*) Traces in the presence of 20-Hz light stimulation with the general muscarinic receptor inhibitor scopolamine (10 µM). [Scale bars, 10 s (*x* axis) and 40 pA (*y* axis).] (*D*) Time course of the frequency of sIPSCs in SPNs ± SEM from WT (*Left*) and p11cKO mice (*Right*) ($n = 20$ neurons for WT and 17 for cKOs; $n = 5$ for scopolamine). $^{****}P < 0.0001$ vs. scopolamine. (*E*) Representative traces showing the frequency of sIPSCs in SPNs from WT and cKO neurons under light stimulation in control and upon the addition of either 10 µM CP93129 (5-HT1B agonist) or 10 µM GR55562 (5-HT1B antagonist). [Scale bars, 10 s (*x* axis) and 40 pA (*y* axis).] (*F*) Histograms of the frequencies of sIPSCs ± SEM in SPNs normalized to baseline frequency in different experimental conditions and genotypes. $^{**}P < 0.01$ vs. cKO. (WT: $n = 20$ for control, $n = 14$ for CP93129, and $n = 8$ for GR55562; p11cKO: $n = 17$ for control, $n = 8$ for CP93129, and $n = 7$ for GR55562 experiments.)

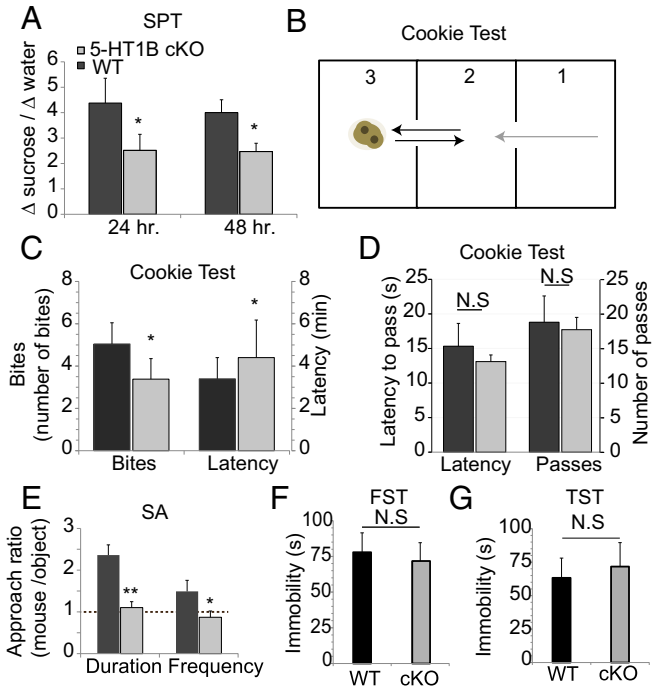

Fig. 5. Loss of 5-HT1B from cholinergic neurons mediates anhedonic behavior. 5-HT1B cKO mice and WT littermates were tested in the following paradigms. (*A*) Sucrose preference test (SPT). Bottles with 2% sucrose and water were weighed after 24 and 48 h of the test. Bars represent means ± SEM (WT, $n = 13$ mice; cKO, $n = 15$ mice; $^*P < 0.05$ vs. WT). (*B–D*) Cookie test. (*B*) Study design. The cookie was placed in compartment 3. The test started when the mouse was placed in compartment 1. The latency to reach the cookie, number of bites, latency to leave the first chamber (gray arrow), and number of passes (black arrows) were determined. (*C*) Bar graph summaries of cookie consumption. Bars represent the number of cookie bites ± SEM (*Left*) and latency for the first contact ± SEM (*Right*) (WT, $n = 16$ mice; cKO, $n = 18$ mice; $^*P < 0.05$ vs. WT). (*D*) Exploratory and motor behaviors during the cookie test. Bars represent the latency to leave the first chamber ± SEM (*Left*). Bars represent the number of passes between compartments ± SEM (*Right*). N.S, not significant. (*E*) Social approach test (SA). Bars represent mean ratios of total interaction time ± SEM and frequency of approaches ± SEM with either an unfamiliar mouse or an object (WT, $n = 12$ mice; cKO, $n = 14$ mice; $^*P < 0.05$ vs. WT; $^{**}P < 0.01$ vs. WT). The dashed line indicates no preference. (*F*) Forced swim test (FST). Bars represent means ± SEM ($n = 15$ mice per group). (*G*) Tail suspension test (TST). Bars represent means ± SEM ($n = 15$ mice per group).

cKO mice; Fig. 3 *F* and *G* and *SI Appendix*, Fig. S2). Hedonic behavior was first determined by preference to consume a 2% (wt/vol) sugar solution. 5-HT1B cKO mice consumed 38% less sugar solution relative to their WT littermates ($P = 0.041$ and $P = 0.027$ after 24 and 48 h, respectively; Fig. 5*A*). We then used the cookie test paradigm, another test that evaluates hedonic behavior (29, 30). Mice were placed in the first compartment and traveled to reach the cookie in the third compartment (Fig. 5*B*), and their latency to approach the cookie as well as the number of cookie bites taken were recorded for each session. 5-HT1B cKO mice manifested a 23% reduction in the number of bites in a chocolate cookie ($P = 0.035$; Fig. 5*C*), as well as a 33% increase in their latency to approach the cookie, relative to WT mice ($P = 0.024$; Fig. 5*C*). Still, motoric and exploratory behaviors were similar in 5-HT1B cKO compared with WT mice, as measured in the cookie test by the latency to exit the first compartment ($P = 0.349$) and by the number of passages between compartments ($P = 0.306$; Fig. 5*D*). These changes in sucrose and cookie consumption are probably not due to the dysfunction in the well-established function of 5-HT1B regulating feeding and metabolism (31), because there were no differences between 5-HT1B cKO mice and their WT littermates in latency to approach ordinary food (in the novelty suppressed feeding paradigm) or in the amount of food and water they consumed ($P = 0.35$ and $P = 0.31$, respectively, relative to WT; *SI Appendix*, Fig. S6).

We next studied a socializing response in 5-HT1B cKO mice. In this paradigm, the mouse is introduced into an arena with an unfamiliar mouse and an object, each enclosed in a small mesh cup. The number and duration of interactions between the subject and each of the cups were recorded. WT mice showed preference to interact with an unfamiliar mouse, whereas 5-HT1B cKO mice spent 63% less time socially interacting ($P = 0.007$; Fig. 5*E*) and had 88% fewer interactions ($P = 0.032$; Fig. 5*E*). Importantly, 5-HT1B cKOs did not manifest despair or helplessness phenotypes, as measured by immobility time in the forced swim test ($P = 0.215$; Fig. 5*F*) or in the tail suspension test ($P = 0.301$; Fig. 5*G*). Together, these data strongly support the idea that 5-HT signaling in vSt ChIs plays a major role in mediating pleasure response.

Discussion

Cholinergic neurons of the vSt and dSt are thought to represent highly homologous neuronal populations. Indeed, only subtle differences were previously reported between these neurons in terms of physiology and morphology (for a review, see ref. 6). No study using a systematic approach to identify differences in molecular characteristics of these ChI populations has been reported. Here we show that (*i*) 5-HT plays opposite roles in vSt and dSt ChIs; (*ii*) differences in 5-HTR expression in the two subpopulations account for these opposite physiological responses to 5-HT; and (*iii*) more specifically, signaling through the 5-HT1B/p11 pathway is involved in the function of vSt ChIs but not in that of dSt ChIs.

The distribution of 5-HT1A and 5-HT1B in the mammalian brain has been studied extensively, but their localization to striatal ChIs has not been described (15, 32–34), likely due to the low abundance of this neuronal population. By using TRAP, we compared the translated mRNA level of 5-HTRs from vSt and dSt ChIs. Expression level suggested that 5-HT1A and 5-HT1B are the predominant 5-HTRs in vSt ChIs. We validated that both 5-HT1A and 5-HT1B proteins are localized to vSt ChIs and confirmed the previously described postsynaptic and presynaptic functions for 5-HT1A and 5-HT1B using electrophysiological recordings. Unlike vSt ChIs, dSt ChIs were depolarized by 5-HT and expressed high levels of 5-HT7. The excitatory effect of 5-HT on dSt ChIs was previously reported, and 5-HT7 together with 5-HT6 and members of the 5-HT2 family were implicated in this response (11, 12). 5-HT2 and 5-HT6 mRNA were not enriched in either ChI population by TRAP analysis. This is in line with a recent study in rats showing that 5-HT6 mRNA is highly expressed in striatal SPNs but not in ChIs (35), and suggests that 5-HT7 may play a major role in the response to 5-HT in dSt ChIs. In contrast to 5-HT7 enrichment in dSt ChIs and 5-HT1A enrichment in vSt ChIs, 5-HT5A isoform was found in both vSt and dSt ChI populations. Because the physiological response to 5-HT is opposite in vSt vs. dSt ChIs, it is likely that 5-HT5A does not play a major role in modulating the excitability of either ChI population.

We found that a loss of 5-HT1B function in cholinergic neurons results in an anhedonic behavioral phenotype, supporting the idea that a serotonergic deficit could lead to a loss of interest in pleasurable activity. In addition to ChIs, striatal 5-HT1B heteroreceptor regulates transmission in glutamatergic nerve terminals innervating the nucleus accumbens (36) and in SPNs innervating either the midbrain (37, 38) or the pallidum (39), whereas 5-HT1B autoreceptor is found in striatal terminals of serotonergic neurons (40). Interestingly, mice bearing a constitutive deletion of 5-HT1B display aggressive behavior and reduced anxiety relative to WT, but do not display anhedonia (28, 31). Furthermore, mice with constitutive loss of either 5-HT1A or 5-HT1B did not display an impairment in preference to sucrose consumption (41). It is likely that 5-HT1B plays opposing roles in different populations of neurons in mediating pleasure response. Constitutive deletion of 5-HT1B could result in impairment in 5-HT1B autoreceptor activity, which would increase 5-HT release from serotonergic terminals. Such an

increase could further activate 5-HT1A in vSt ChIs, which could contribute to hedonic behavior.

p11 is highly expressed in vSt ChIs of the striatum of mice and humans (5), and it is involved in mediating the function of 5-HT1B but not that of 5-HT1A. This is in line with our previous findings of a functional interaction between p11 and 5-HT1B, but not with 5-HT1A (19, 20). We previously showed that deletion of p11 from cholinergic neurons in mice results in anhedonia as well as despair-like behaviors, and that restoration of p11 in vSt ChIs reversed these behaviors (5, 21). The present study clearly associates 5-HT signaling in vSt ChIs specifically with pleasure response, and indicates that p11 in vSt ChIs can mediate different aspects of emotional behavior by multiple mechanisms that need not be mediated by 5-HT signaling. Future studies should aim to elucidate molecular mechanisms in vSt ChIs underlying the 5-HT–independent components of mood control.

Materials and Methods

A full description of the materials and methods, including perforated-patch recordings, stereotaxic injections and optogenetic recordings, microdialysis, mRNA expression analysis, immunohistochemistry, and animal behavioral assays can be found in *SI Appendix, Materials and Methods*.

Animals. All procedures were carried out in accordance with the NIH guidelines and were approved by the Animal Care and Use Committees of The Rockefeller University. Animals were crossed with C57/Bl6N mice and housed in a 12-h light/dark interval with food and water ad libitum. $ChAT^{Cre}$ (GM60) mice were maintained heterozygous and, where appropriate, littermate $ChAT^{Cre}$-negative mice were used as WT. Mice with a conditional deletion of 5-HT1B were generated by introducing flanked loxP sites in the promoter and exon of *htr1b* and inserting human growth hormone polyadenylation signal 3′ of the gene. These animals were crossed with $ChAT^{Cre}$ to generate 5-HT1B cKO ($htr1b^{flox/flox}$; $ChAT^{Cre+/-}$), which were maintained on a C57/Bl6N background. $ChAT^{BacTRAP}$ (DW-167) were maintained on a C57/Bl6N background and heterozygous. $ROSA26^{Tdtomato}$ mice were maintained on a C57/Bl6J background and heterozygous, and $ChAT^{EGFP}$ (GH-293) mice were maintained on a C57/Bl6N background and heterozygous.

Statistical Analysis. Unless mentioned otherwise, all data are expressed as means ± SD. Perforated-patch recordings, quantitative PCR, and most behavioral tests were statistically analyzed using two-tailed paired *t* test. Analysis of ACh levels used one-way ANOVA with post hoc two-tailed unpaired *t* test. Analysis of the frequency of sIPSCs used repeated measures one-way ANOVA with post hoc Dunnett's test, and the effects of drugs on the frequency of sIPSCs or on membrane potential both used one-way ANOVA with post hoc Tukey test. Sucrose preference test used one-way ANOVA followed by Bonferroni test. Analyses of immunolabeling as well as for the number of bites in the cookie test were performed by Mann–Whitney test. Statistical significance was determined using GraphPad Prism 5. $P < 0.05$ was considered significant.

ACKNOWLEDGMENTS. We thank Jodi Gresack for valuable suggestions on behavioral studies, and Angus Nairn, Victor Bustos, and Marc Flajolet for their comments on the manuscript. This work was supported by the National Institute of Drug Abuse of the National Institutes of Health under Award DA010044 (to P.G.), the JPB Foundation (P.G.), and the US Army Medical Research Materiel Command under Awards W81XWH-14-1-0130 (to Y.S.) and W81XWH-09-1-0401 (to Y.S.).

1. Bolam JP, Wainer BH, Smith AD (1984) Characterization of cholinergic neurons in the rat neostriatum. A combination of choline acetyltransferase immunocytochemistry, Golgi-impregnation and electron microscopy. *Neuroscience* 12(3):711–718.
2. Goldberg JA, Wilson CJ (2010) The cholinergic interneurons of the striatum: Intrinsic properties underlie multiple discharge patterns. *Handbook of Basal Ganglia Structure and Function*, eds Steiner H, Tseng KY (Elsevier, Chicago), pp 133–149.
3. Witten IB, et al. (2010) Cholinergic interneurons control local circuit activity and cocaine conditioning. *Science* 330(6011):1677–1681.
4. Apicella P (2002) Tonically active neurons in the primate striatum and their role in the processing of information about motivationally relevant events. *Eur J Neurosci* 16(11):2017–2026.
5. Warner-Schmidt JL, et al. (2012) Cholinergic interneurons in the nucleus accumbens regulate depression-like behavior. *Proc Natl Acad Sci USA* 109(28):11360–11365.
6. Gonzales KK, Smith Y (2015) Cholinergic interneurons in the dorsal and ventral striatum: Anatomical and functional considerations in normal and diseased conditions. *Ann N Y Acad Sci* 1349:1–45.
7. Beaudoin-Gobert M, Sgambato-Faure V (2014) Serotonergic pharmacology in animal models: From behavioral disorders to dyskinesia. *Neuropharmacology* 81:15–30.
8. Müller CP, Homberg JR (2015) The role of serotonin in drug use and addiction. *Behav Brain Res* 277:146–192.
9. El Yacoubi M, Dubois M, Gabriel C, Mocaër E, Vaugeois JM (2011) Chronic agomelatine and fluoxetine induce antidepressant-like effects in H/Rouen mice, a genetic mouse model of depression. *Pharmacol Biochem Behav* 100(2):284–288.
10. Adell A, Carceller A, Artigas F (1991) Regional distribution of extracellular 5-hydroxytryptamine and 5-hydroxyindoleacetic acid in the brain of freely moving rats. *J Neurochem* 56(2): 709–712.
11. Bonsi P, et al. (2007) Endogenous serotonin excites striatal cholinergic interneurons via the activation of 5-HT 2C, 5-HT6, and 5-HT7 serotonin receptors: Implications for extrapyramidal side effects of serotonin reuptake inhibitors. *Neuropsychopharmacology* 32(8):1840–1854.
12. Blomeley C, Bracci E (2005) Excitatory effects of serotonin on rat striatal cholinergic interneurones. *J Physiol* 569(Pt 3):715–721.
13. Doyle JP, et al. (2008) Application of a translational profiling approach for the comparative analysis of CNS cell types. *Cell* 135(4):749–762.
14. Bennett BD, Callaway JC, Wilson CJ (2000) Intrinsic membrane properties underlying spontaneous tonic firing in neostriatal cholinergic interneurons. *J Neurosci* 20(22):8493–8503.
15. Boschert U, Amara DA, Segu L, Hen R (1994) The mouse 5-hydroxytryptamine1B receptor is localized predominantly on axon terminals. *Neuroscience* 58(1):167–182.
16. Ghavami A, et al. (1999) Differential addressing of 5-HT1A and 5-HT1B receptors in epithelial cells and neurons. *J Cell Sci* 112(Pt 6):967–976.
17. Peroutka SJ (1988) 5-Hydroxytryptamine receptor subtypes: Molecular, biochemical and physiological characterization. *Trends Neurosci* 11(11):496–500.
18. Rada PV, Mark GP, Hoebel BG (1993) In vivo modulation of acetylcholine in the nucleus accumbens of freely moving rats: I. Inhibition by serotonin. *Brain Res* 619(1-2):98–104.
19. Svenningsson P, et al. (2006) Alterations in 5-HT1B receptor function by p11 in depression-like states. *Science* 311(5757):77–80.
20. Warner-Schmidt JL, et al. (2009) Role of p11 in cellular and behavioral effects of 5-HT4 receptor stimulation. *J Neurosci* 29(6):1937–1946.
21. Alexander B, et al. (2010) Reversal of depressed behaviors in mice by p11 gene therapy in the nucleus accumbens. *Sci Transl Med* 2(54):54ra76.
22. Alger BE, Nagode DA, Tang AH (2014) Muscarinic cholinergic receptors modulate inhibitory synaptic rhythms in hippocampus and neocortex. *Front Synaptic Neurosci* 6:18.
23. de Rover M, Lodder JC, Kits KS, Schoffelmeer AN, Brussaard AB (2002) Cholinergic modulation of nucleus accumbens medium spiny neurons. *Eur J Neurosci* 16(12):2279–2290.
24. Nagode DA, Tang AH, Karson MA, Klugmann M, Alger BE (2011) Optogenetic release of ACh induces rhythmic bursts of perisomatic IPSCs in hippocampus. *PLoS One* 6(11):e27691.
25. Nelson AB, et al. (2014) Striatal cholinergic interneurons drive GABA release from dopamine terminals. *Neuron* 82(1):63–70.
26. Sugam JA, Saddoris MP, Carelli RM (2014) Nucleus accumbens neurons track behavioral preferences and reward outcomes during risky decision making. *Biol Psychiatry* 75(10):807–816.
27. Varrone A, et al. (2015) 5-HT1B receptor imaging and cognition: A positron emission tomography study in control subjects and Parkinson's disease patients. *Synapse* 69(7):365–374.
28. Saudou F, et al. (1994) Enhanced aggressive behavior in mice lacking 5-HT1B receptor. *Science* 265(5180):1875–1878.
29. Isingrini E, et al. (2010) Association between repeated unpredictable chronic mild stress (UCMS) procedures with a high fat diet: A model of fluoxetine resistance in mice. *PLoS One* 5(4):e10404.
30. Surget A, et al. (2011) Antidepressants recruit new neurons to improve stress response regulation. *Mol Psychiatry* 16(12):1177–1188.
31. Brunner D, Buhot MC, Hen R, Hofer M (1999) Anxiety, motor activation, and maternal-infant interactions in 5HT1B knockout mice. *Behav Neurosci* 113(3):587–601.
32. Riad M, et al. (2000) Somatodendritic localization of 5-HT1A and preterminal axonal localization of 5-HT1B serotonin receptors in adult rat brain. *J Comp Neurol* 417(2):181–194.
33. Kia HK, et al. (1996) Immunocytochemical localization of serotonin1A receptors in the rat central nervous system. *J Comp Neurol* 365(2):289–305.
34. Sari Y, et al. (1997) Light and electron microscopic immunocytochemical visualization of 5-HT1B receptors in the rat brain. *Brain Res* 760(1-2):281–286.
35. Helboe L, Egebjerg J, de Jong IE (2015) Distribution of serotonin receptor 5-HT6 mRNA in rat neuronal subpopulations: A double in situ hybridization study. *Neuroscience* 310:442–454.
36. Morikawa H, Manzoni OJ, Crabbe JC, Williams JT (2000) Regulation of central synaptic transmission by 5-HT(1B) auto- and heteroreceptors. *Mol Pharmacol* 58(6):1271–1278.
37. Ding S, Li L, Zhou FM (2015) Robust presynaptic serotonin 5-HT(1B) receptor inhibition of the striatonigral output and its sensitization by chronic fluoxetine treatment. *J Neurophysiol* 113(9):3397–3409.
38. Stanford IM, Lacey MG (1996) Differential actions of serotonin, mediated by 5-HT1B and 5-HT2C receptors, on GABA-mediated synaptic input to rat substantia nigra pars reticulata neurons in vitro. *J Neurosci* 16(23):7566–7573.
39. Querejeta E, Oviedo-Chávez A, Araujo-Alvarez JM, Quiñones-Cárdenas AR, Delgado A (2005) In vivo effects of local activation and blockade of 5-HT1B receptors on globus pallidus neuronal spiking. *Brain Res* 1043(1-2):186–194.
40. De Groote L, Olivier B, Westenberg HG (2003) Role of 5-HT1B receptors in the regulation of extracellular serotonin and dopamine in the dorsal striatum of mice. *Eur J Pharmacol* 476(1-2):71–77.
41. Bechtholt AJ, Smith K, Gaughan S, Lucki I (2008) Sucrose intake and fasting glucose levels in 5-HT(1A) and 5-HT(1B) receptor mutant mice. *Physiol Behav* 93(4-5):659–665.
42. Rosen GD, et al. (2000) The Mouse Brain Library @ www.mbl.org. *Int Mouse Genome Conference* 14:166. Available at www.mbl.org.